Process Intensification of the Continuous Synthesis of Bio-derived Monomers for Sustainable Coatings using a Taylor Vortex Flow Reactor

Matthew D. Edwards,[a] Matthew T. Pratley,[a] Charles M. Gordon,[b] Rodolfo I. Teixeira,[a] Hamza Ali,[a] Irfhan Mahmood,[a] Reece Lester,[a] Ashley Love,[a] Johannes G. H. Hermens,[c] Thomas Freese,[c] Ben L. Feringa,[c] Martyn Poliakoff,[a] and Michael W. George[a]*

[a] *School of Chemistry, University of Nottingham, University Park, Nottingham, NG7 2RD, UK,*
[b] *Scale-up Systems Ltd., 23 Shelbourne Road, Dublin 4, D04 PY68, Ireland*
[c] *Advanced Research Centre CBBC, Stratingh Institute for Chemistry, Faculty of Science and Engineering, University of Groningen, Nijenborgh 4, Groningen, 9747 AG, Netherlands.*

Keywords: flow chemistry, photo-oxidation, biomass, sustainability, coatings
e-mail: michael.george@nottingham.ac.uk

ABSTRACT

We describe the optimization and scale-up of two consecutive reaction steps in the synthesis of bio-derived alkoxybutenolide monomers that have been reported as potential replacements for acrylate-based coatings (*Sci. Adv*., **2020**, *6*, eabe0026). These monomers are synthesized by (i) oxidation of furfural with photo-generated singlet oxygen followed by (ii) thermal condensation of the desired 5-hydroxyfuranone intermediate product with an alcohol, a step which until now has involved a lengthy batch reaction. The two steps have been successfully telescoped into a single kilogram-scale process without any need to isolate the 5-hydroxyfuranone between the steps. Our process development involved FTIR reaction monitoring, FTIR data analysis via 2D-visualization and two different photo-reactors (i) a semi-continuous photo-reactor based on a modified rotary evaporator where FTIR and 2D-correlation spectroscopy (2D-COS) revealed the loss of the methyl formate co-product and (ii) our fully continuous Taylor Vortex photo-reactor which enhanced the mass transfer and permitted the use of near-stoichiometric equivalents of O_2. The use of inline FTIR monitoring and modelling greatly accelerated process optimization in the Vortex reactor. This led to scale up of the photo-oxidation with an 85% yield and a projected productivity of 1.3 kg day^{-1}, with a space time yield of 0.06 mol day^{-1} mL^{-1}. Higher productivities could be achieved whilst sacrificing yield; e.g. 4 kg day^{-1} at 40% yield. The second step, the thermal condensation of 5-hydroxyfuranone, was transformed from a 20 h batch reflux reaction to a < 1 minute thermal flow reaction in a reactor only 3 mL in volume operating at 200 ^{o}C with projected productivities of >700 g day^{-1}. Proof of concept for telescoping the two steps was established with an overall two-step yield of 67%, producing a process with projected productivity of 1.1 kg day^{-1} of the methoxybutenolide monomer without any purification of the 5-hydroxyfuranone intermediate.

INTRODUCTION

Our reliance on polymers in daily life is currently dependent on the availability of affordable fossil fuel feedstocks.[1] There is a growing movement to develop polymers and materials that are sourced from renewable sources to drive towards Net Zero production and a circular economy.[2] Monomers derived from glycerol,[3] terpenes,[4–6] and vegetable oils[7,8] can be used for the manufacture of a wide variety of sustainable materials and products including elastomers, plastics, resins, and coatings. There is increasing interest in using biomass and lignocellulose as feedstocks[9,10] and of particular relevance to this paper several bio-based acrylate resins for coating applications have been prepared.[11] Not only are these coatings favorable for environmental reasons, but bio-based acrylates have also shown to have superior properties to their oil-based counterparts.[12]

Furfural, is a common feedstock, derived from lignocellulosic biomass, which has been used to produce bio-based acrylate monomers and has recently attracted interest as a platform chemical, both due to its versatility[13] and low cost.[14] The application of alkoxybutenolide monomers, derived from furfural, as high-performance coatings has recently been demonstrated.[15,16] Furfural, **1**, undergoes a [4+2] cycloaddition with photochemically generated singlet oxygen ($^1O_2$) and forms γ-hydroxybutenolide, **2**, in presence of methanol, which can be followed by a thermal condensation reaction in the presence of a suitable alcohol to form the desired alkoxybutenolide monomer, **3** (Figure 1).[17] This process has potential as a bio-derived replacement for acrylate monomers in the coatings market in order to avoid reliance on oil derived hydrocarbons.[18] In this paper we focus on new approaches for scaling-up the consecutive reaction steps to >1 kg day^{-1} as a further demonstration of the potential of bio-based feedstocks and to readily access quantities of monomers for advanced coatings testing.

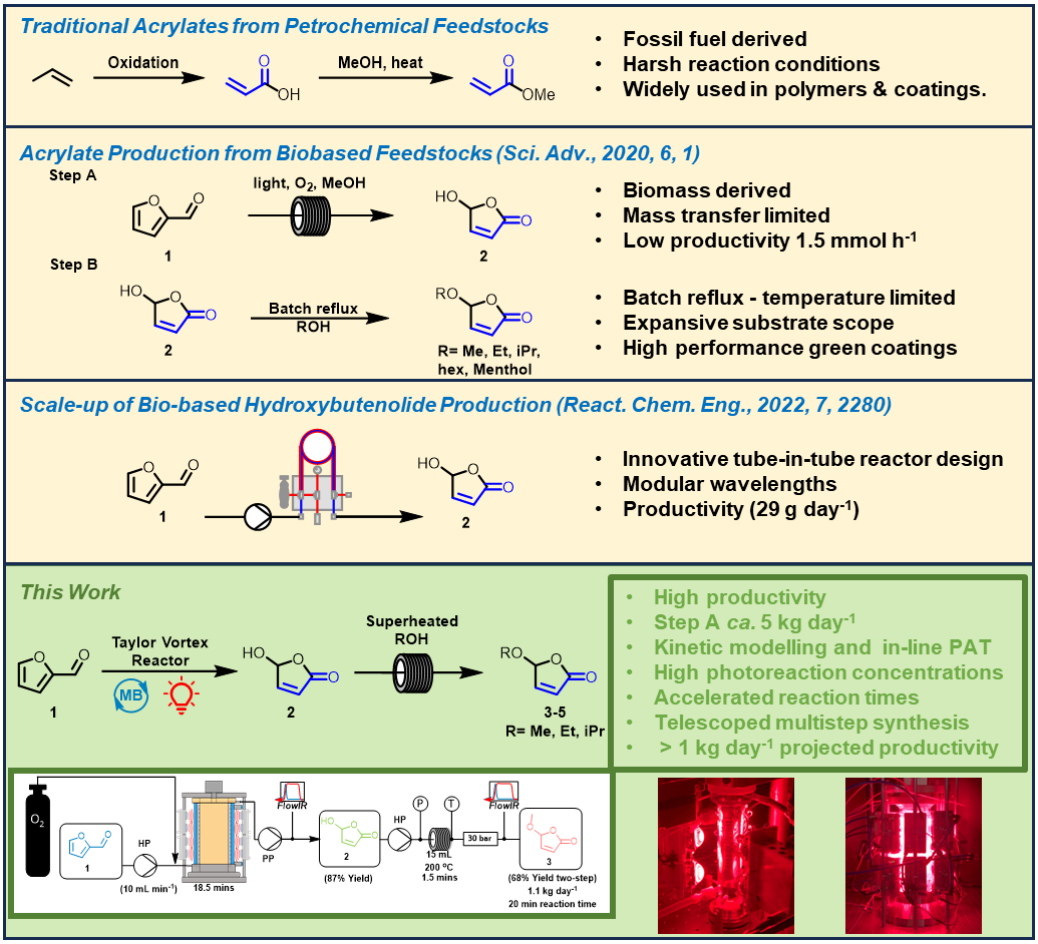

Figure 1. The journey from traditional acrylates (from petroleum feedstock) to furfural and biomass derived monomers highlighting the technical innovations by Hermens *et al.* and our further upscaling of this process.

The photo-oxidation step was the limiting step in terms of batch chemical processing because batch photo-oxidation is difficult to scale due to light penetration[19] and oxygen mass transfer from gas to solution. Continuous flow photo-oxidation provides an attractive alternative for addressing these issues, particularly light penetration, but upscaling photo-oxidation reactions using classical tubular flow reactors results in segmented gas-liquid flow and the resulting poor mass transfer can hinder scale-up.[20] There have been several examples of innovative flow reactor designs that enhance multi-phase mass transfer using membranes to deliver gas microbubbles.[21,22] Other designs such as the continuous spinning disk[23] or continuous Taylor Vortex reactor[24,25] were developed with active mixing using a rotor-stator design, generating efficient multi-phase mass transfer often resulting in reduced reaction times in a process platform that largely decouples the mixing from the residence time.

The batch condensation was previously reported using ambient pressure batch conditions which were dictated by the solvent selection and upscaling these thermal transformations can be problematic with a large manufacturing footprint and the associated problems with heat transfer.[26] Flow chemistry enables access of an expanded process window by superheating classical organic

solvents above their boiling points with little reactor modification required.[27–32] Superheated flow chemistry has also enabled the removal of harsh acid catalysts needed to overcome the activation energy of some processes.[33] There is increased activity in developing linked flow reactions into telescoped sequences since such operation has a number of advantages including increasing the efficiency of the process, and potentially minimizing/avoiding handling of hazardous intermediates.[34]

In this paper, we have investigated the PhotoVortex reactor for the intensification and scale up of the photo-oxidation of furfural, **1**, with $^1O_2$ and have undertaken the first flow synthesis of **3-5** using superheated reaction solvents to accelerate the reaction. We have also carried out a preliminary study towards the synthesis of **3** as a telescoped multistep flow process with a potentially significant reduction in solvent waste, by eliminating intermediate isolation steps.

RESULTS AND DISCUSSION

Photo-oxidation in a 'PhotoVap' Reactor.

Preliminary studies were carried out on the photo-oxidation of furfural, **1,** as outlined in Figure 1 using a modified rotatory evaporator (PhotoVap).[35] The PhotoVap employs a thin film of reaction solution that acts as a large surface over which the light can penetrate and O_2 can transfer into the solution, see Fig. 2. A similar reactor was used in the previous report[20] but our approach differs in two principal ways (i) a computer-controlled Arduino board automates the semi-continuous operation of the evaporator and two pumps, which can be programmed for a fresh aliquot and (ii) the LEDs are multi-wavelength rather than monochromatic which enables a range of different photosensitizers to be used without any need to change the LEDs. This arrangement allows irradiation of the thin film for a fixed amount of time before removing and replacing the solution with a fresh aliquot.

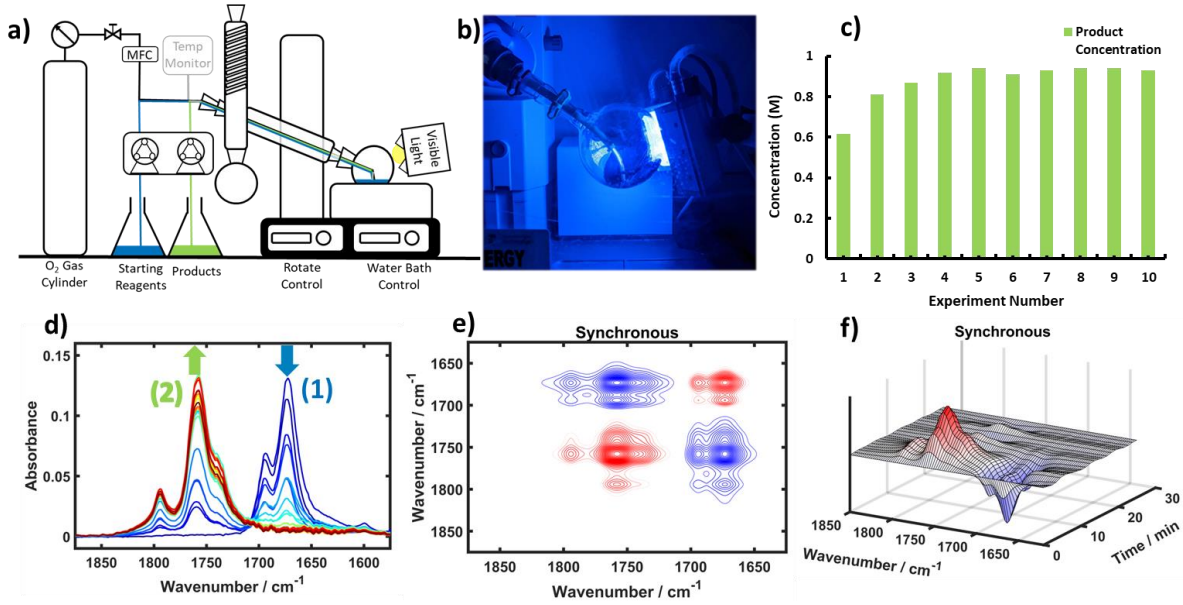

Figure 2. (a): Schematic of the PhotoVap reactor operating in semi-continuous mode. The flow of O_2 is controlled via a Mass Flow Controller (**MFC**) and the peristaltic pumps pumping solutions in and out of the reactor at set time intervals (controlled by an Arduino Board). Reaction temperature was monitored via a Type K thermocouple which sits at the bottom of the reaction flask. (b): Photo of the PhotoVap in operation (taken through a blue filter with the cooling bath removed for the photo). (c): Plot of the product concentration stabilizing over the course of 3.5-hour semi-continuous experiment (10 cycles) with an irradiation time of 20 minutes; conversions and yields which were monitored by NMR. (d): Offline IR measurements showing the consumption of **1** and formation of (**2**) over time. (e): Synchronous 2D COS enabling the visualization of the conversion of **1** → **2**, as well as the absence of methyl formate co-product evident in the negatively correlated cross peaks. (f): Synchronous Perturbation Correlation Moving Window 2D analysis (PCMW2D) of the offline IR spectra. Here the perturbation is the reaction time, peaks of opposite sign correlate negatively at each slice of the time axis, allowing for clear observation of the reaction proceeding and the respective rates of this process for the conversion of **1** → **2,** again there is a clear absence of the methyl formate peak.

Figure 2(a) depicts a schematic of the PhotoVap and we find this arrangement proves to be a stable and robust set-up with batches being processed reproducibly under full computer control. Previously, a productivity of 30 mmol h^{-1} has been reported for the desired hydroxyfuranone, **2**, in batch mode with 8x100 W LEDs with quantitative yields when a positive pressure of O_2 was supplied to the system via a balloon.[20] In our experiments, we enhanced gas-liquid mass transfer by bubbling O_2 gas through the pool of liquid at the bottom of the rotating flask. Initial experiments were undertaken without cooling and the progress of the reaction was monitored by off-line FTIR, Figure 2(d). It was clear that the conversion of starting material to product can easily be monitored but there was an absence of strong signals from formation of the expected methyl formate by-product (1732 cm-

[1]). The absence of methyl formate in the FTIR can be visualized by 2D-correlation spectroscopy (2D-COS)[36] with missing cross peaks in the synchronous correlation spectrum, along with its absence in the synchronous Perturbation Correlation Moving Window 2D analysis (PCMW2D). PCMW2D is particularly useful in reaction monitoring as it allows for the determination of how the spectral variation depends on the perturbation applied, in this case reaction time, however the perturbation could also be in the form of adjustments to the flow conditions, such as temperature or pressure. The result is consistent with the methyl formate (b.p. 32 °C) being lost by evaporation under these conditions and subsequent experiments in the PhotoVap were undertaken with active cooling to *ca.* 15 °C. The PhotoVap was operated for 3.5 hours (10 cycles) with an irradiation time of 20 minutes per cycle and this gave high conversions and yields (92%). Initial product concentrations were lower than might be expected, but this was only due to a dilution effect which is commonly seen in flow chemistry when reactors or outlet pumps have been primed with pure solvent at the start of the experiment. The conversion stabilized after four cycles. Despite using lower power LEDs (360 W) than in the previous report, we achieved 28 mmol h^{-1} with less than half the power indicating that gas-liquid contacting is a critical factor towards efficient photo-oxidation reactions. Taking the PhotoVap forward, however, raises potential safety limitations regarding the scale-up of the reaction/reactor with bubbling O_2 into the reaction solution in the presence of large free volumes of gaseous O_2.

Photo-oxidation in the Small Taylor Vortex Reactor

We have recently reported the use of Taylor Vortex reactors for both photochemistry[24,25] and electrochemistry.[37,38] The photochemical version, the PhotoVortex, ensures highly efficient gas-liquid micro-mixing, which enables lower equivalents of gaseous O_2 to be used with very small volumes of gaseous O_2. Most of our experiments are designed to be near-stoichiometric so that during periods of long-term operation > 85% of the introduced O_2 gas is completely consumed by the reaction. As used here, the smaller PhotoVortex Reactor consists of a transparent Pyrex-jacketed tube that is sealed at the bottom and contains a polished stainless-steel cylindrical rotor with a narrow bore running coaxially through its center. We initially used our smaller PhotoVortex with a 1 mm annular gap size between the rotor and the glass tube, giving an irradiated volume of *ca.* 8 mL. The PhotoVortex used in this paper was modified slightly from our previous reports[24,25] by using newly designed LED blocks. (3 x 200 W blocks), equipped with lenses which act both to focus the LED output and to protect the LED chips. The output wavelength of these LEDs (660 nm) overlaps with the absorption band of methylene blue in methanol (λ_{max} = 654 nm). In these experiments, the O_2 gas was dosed via a T-junction at the reactor inlet as shown in Figure 3(a).

Building upon the offline IR measurements used in the experiments in the PhotoVap above, we have employed real-time IR reaction monitoring with a custom-made flow cell and quantitative IR spectra monitoring was achieved were converted to concentration using a series of product calibration standards and with multivariate curve resolution (MCR) and partial least squares (PLS) models. Initial reaction conditions were obtained from literature and a methylene blue concentration of 2 mM was chosen due to the inner-filter effects observed by Hermens *et al*.[20] For proof-of-concept with the new LEDs, the reaction was carried out with 0.5 M of **1**, and the amount of O_2 was initially varied between 1.05-1.2 eq.

Table 1. Optimization table for the photo-oxidation of furfural in the Vortex Reactor 0.5 M – 2 M highlighting the trade-off between high yield and high productivity.

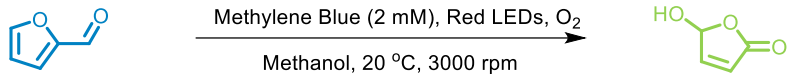

1 2

Entry	[Substrate, 1] (M)	Space time (min)	O_2 Equiv.	Conv. of 1 (%)[a]	Yield of 2 (%)[a]	Productivity (g day^{-1})[b]
1	0.5	8	1.2	95	92	66
2	**1**	**8**	**1.2**	**98**	**95**	**140**
3	1	4.	1.2	95	77	220
4	1	2.7	1.2	87	60	260
5	1	8	2.5	93	88	130
6	1	4	2.5	85	80	230
7	1	2.7	2.5	74	69	300
8	1	16	2.5	98	96	70*
9	**1.5**	**2.7**	**2.5**	**75**	**64**	**410**
10	2	2.7	^2	55	46	397

a) NMR yields calculated using 1,3,5-trimethoxybenzene as the internal standard, b) Projected productivity over 24 hours of operation * Fouling observed ^flow rate limit of the mass flow controller.

Entry 1 in Table 1 shows that the reaction proceeded under these conditions with high efficiency. The concentration was then doubled to match the PhotoVap experiments and Table 1, entry 2 shows an equally efficient conversion and yield compared to the previous experiments using the PhotoVap despite reduced reaction times of 8 min. This is consistent with the more efficient mass-transfer we have observed in the PhotoVortex.

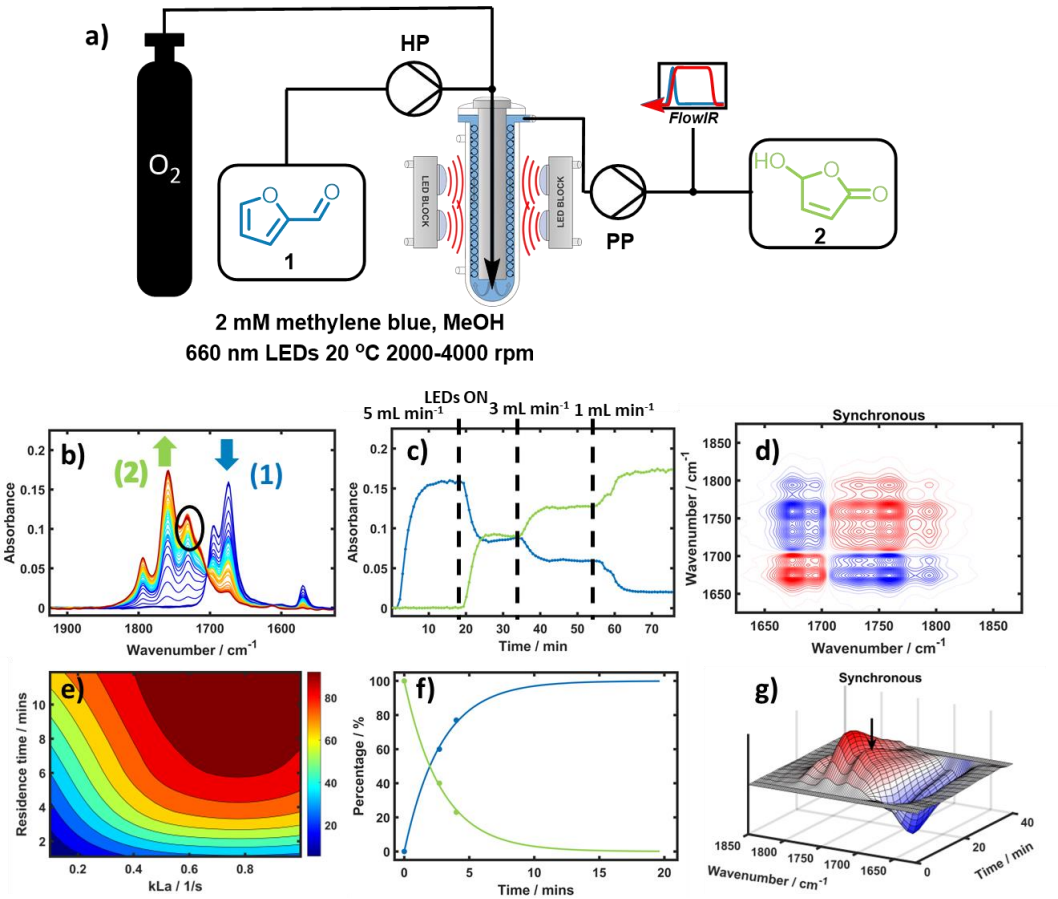

Figure 3. (a): Schematic of the photochemical vortex reactor including inline FTIR analysis at the outlet of the reactor. HP is HPLC pump and PP is Peristaltic pump (b): ReactIR spectra, 1900 cm^{-1} to 1600 cm^{-1} used to monitor the photochemical oxidation of furfural **1** in MeOH solution at 20 °C; spectra are colored blue (start of reaction) to red (end of reaction); methyl formate was observed at *ca.* 1732 cm^{-1} in the black circle. (c): monitoring of consumption of furfural (blue) and formation of 5-hydroxyfuranone (green) at decreasing flowrates (5 mL min^{-1}, 3 mL min^{-1}, and 1 mL min^{-1}) showing the positive effect of increased residence time on product formation. (d): Synchronous 2D-COS showing formation of methyl formate by clear cross peaks at ca. 1732 cm^{-1} as well as the conversion of **1** → **2**, ((e): Contour plot generated with Reaction Lab software showing the influence of residence time and mass transfer coefficient, k_La, on the yield of hydroxyfuranone, **2**. (f): Plot of the Reaction Lab model *versus* experimental data points showing the good fit of the model. (g): Synchronous PCMW2D of the real-time IR spectra. Again, the perturbation is the reaction time and allows for the observation of the reaction proceeding, however, in this case the methyl formate peak is clearly visible and is concomitant with the product formation.

Figure 3(c) shows preliminary results for the inline FTIR reaction monitoring of the consumption of furfural and formation of 5-hydroxyfuranone at different flowrates (5 mL min^{-1}, 3 mL min^{-1}, and 1 mL min^{-1}) using a rotor speed of 3000 rpm and as expected, increasing the residence time can be used to increase product formation. Apart from the concentration, and therefore yield provided using our MCR model, the FTIR data permitted the identification of the point when steady-steady operation had been re-established following a change in reaction conditions. We were then able to

shorten our optimization time using inline FTIR by using the steady state readout which was observed after *ca.* three space times rather than waiting much longer for three system volumes of reaction mixture to pass through the whole reactor assembly. In these experiments, methyl formate IR bands are clearly observed by inline monitoring, Figure 3(b), and are even more striking in the 2D-COS analysis with clear cross-peaks and correlation peaks, Figure 3(d & g). This contrasts with the initial experiment in the PhotoVap, Figure 2(e & f).

We have generated a crude kinetic model for the photo-oxidation of **1** → **2** under our reaction conditions using the commercially available software package Reaction Lab.[39] Our aim was to use this software to reduce the number of experiments required to obtain purposeful information from the model. In particular, we were interested to learn how well a kinetic model could predict the reactor performance based on reaction profiles determined from very limited amounts of experimental data. Once the initial model had been generated, further data points could be added to improve the model in an iterative process. In the Reaction Lab model, we defined the irradiated reactor volume as the overall volume, and defined an individual scenario for each set of starting conditions (e.g. 2-furfural concentration, O_2 pressure, rotation speed/k_La). Each experimental data point was determined by running the reaction at different flow rates. The general methodology for collecting reaction profiles from a flow reactor for kinetic modelling have been described previously.[40] The workflow for completing a Reaction Lab model can be found in the Supporting Information.

Briefly, we started by taking two data points from our initial experiments (Table 1, Entries 3 & 4) with a rotation speed of 3000 rpm. Photon flux was calculated with calibrated Ocean Optics fibers in 'Absolute Irradiance' mode. However, the most important assumption that we found to affect the model was the mass transfer coefficient (k_La) and this value was set at 1 s^{-1}, which we used to indicate a relatively well-mixed gas-liquid system. The preliminary model fitted the initial data well (Figure 3(e)) and found that the rate-determining step was the reaction of photochemically generated $^1O_2$ with **1**. An optimization was then carried out with an objective target function of 95% yield and the model predicted that this would occur with a residence time of 8.5 min.

Using this initial model, we investigated the performance of the PhotoVortex reactor by obtaining experiment results for three different rotation speeds (0, 1000, and 3000 rpm) and carrying out a simulation with a fixed liquid flowrate of 1 mL min^{-1} and 1.2 eq. O_2, Reaction Lab was able to display the influence of rotation speed at a given residence time (end time in Reaction Lab output) providing an output of predicted k_La. Experimentally, with no rotation, a yield of 22% was observed, corresponding to an estimated k_La value of 0.15 s^{-1}. As the rotation speed increased to 1000 and 3000 rpm, the formation of Taylor vortices was achieved, yields of 68% and 95% were obtained

corresponding to k_La values of 0.3 s^{-1} and >0.5 s^{-1}, respectively. Positively, the addition of two further experimental data points to the model improved the 'Optimization' function and for a yield of 95% an end time of 8.3 min was estimated. Model validation was achieved from the small DOE study whereby a 95% yield was achieved with a space time of 8 min (1 mL min^{-1}).

In an effort to maximize the productivity of this reaction, we aimed to increase the concentration further to 1.5 M and 2 M (Table 1, entries 9 & 10) where we observed a small drop off in yield due to the elevated oxygen flowrates required to satisfy the reaction stoichiometry. The detrimental effect on the reaction was due to instability of vortices and the resulting reactor bypass of slugs of gas. Nevertheless, reasonable yields of 64 % and 46 % were still achieved by increasing the equivalents of oxygen further in the cases where flow instability was already an issue e.g. (Table 1, entries 4 & 7). With these conditions, a projected maximum productivity of *ca.* 400 g day^{-1} was achieved with a 64% yield in a reactor with an irradiated volume of *ca.* 8 mL, or a lower productivity 140 g day^{-1} but with a much higher 95% yield (3 mL min^{-1} and 1 mL min^{-1} respectively and 3000 rpm).

Intensification of the Thermal Condensation of Hydroxyfuranone to Alkoxybutenolides

In this section, we investigate how the thermal condensation reaction of **2** with MeOH could be sufficiently accelerated in a high-temperature tubular reactor to match the productivity of the continuous photo-oxidation step in the PhotoVortex reactor obtained above. Long reaction times of *ca.* 20 hours under reflux conditions have previously been reported in batch,[20] which is problematic for the integration into a two-step (photochemical + thermal) continuous process. Therefore, we have exploited the expanded process window available in a pressurized continuous flow that in order to accelerate the conversion of **2** → **3**, reducing the reaction time for this second step whilst maintaining a small reactor footprint (Figure 4(a)).

Initial reactions were carried out at 0.1 M in a 3 mL stainless steel tubular reactor and we investigated the relationship between temperature and residence time on the formation of **3** while monitoring the system pressure to ensure that no precipitation or blockage of the reactor occurred. Conversions and yields were monitored *via* NMR and can be visualized in the bar plot (Figure 4(d)). This plot shows that, as the temperature increases, a step-change occurs at 200 °C and 1-2 mL min^{-1}, whereby the yield begins to increase as the residence time is decreased (Entries 7 & 8). It was for this reason that we decided to limit the upper boundary reaction temperature to 200 °C while seeking to scale up this process. Once again, the application of inline FTIR proved to be highly significant, demonstrating its effectiveness in screening and optimization of this thermal condensation, Figure 4(e).

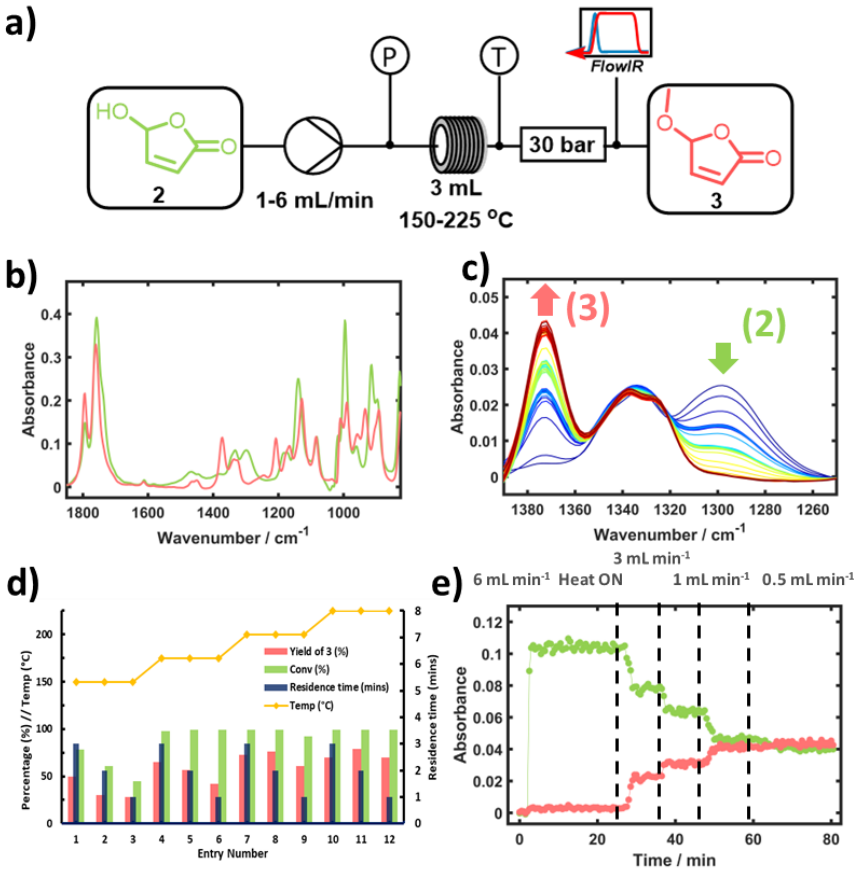

Figure 4. (a): Simplified process schematic for the thermal condensation reaction in a stainless-steel tubular reactor; P, pressure gauge; T, thermocouple. (b): FTIR spectra of pure individual components 5-hydroxyfuranone (green) and 5-methoxybutenolide (rose). (c): Zoomed section of a series of ATR- FTIR spectra showing how the consumption of **2** and formation of **3** can be easily monitored. (d): Bar chart of the data from initial experiments at 0.1 M, highlighting the influence of temperature on reaction yield entries 7&8 show increased yields despite shorter residence times (e): FTIR data recorded at a reaction temperature of 150 °C, showing the effect of different flow rates on the consumption of **2** (green) and formation of **3** (rose).

Further scale-up of the thermal condensation reaction was achieved by optimizing the balance between flowrate and temperature as the concentration of the reaction was to be increased to 1 M (Table 2). As expected, as the concentration of **2** was increased, the reaction proceeded more favorably and as a result required a lower reaction temperature to achieve acceptable yields. Productivities for this condensation matched and even exceeded those of the photo-oxidation of **1** in the PhotoVortex reactor outlined above and at a flowrate of 6 mL min $^{-1}$ a projected productivity of >700 g day^{-1} was achieved in our small flow reactor 3 mL).

Table 2. Optimization table for thermal condensation of 5-hydroxyfuranone at 1 M

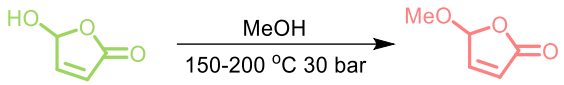

2 3

Entry	Temp (°C)	Spacetime (mins)	Conv. of 2 (%)	Yield of 3 (%)	Productivity (g day^{-1})	mmol hr^{-1}
1	150	3	91	72	120	43
2	150	1.5	75	61	200	73
3	150	1	68	53	260	95
4	175	3	92	79	130	47
5	175	1.5	91	84	270	100
6	175	1	86	73	360	130
7	200	3	98	80	130	48
8	200	1.5	96	82	270	100
9	200	1	95	81	400	140
10	200	0.8	92	78	510	190
11	200	0.6	89	76	630	230
12	200	0.5	86	74	730	270

Conversion and yield monitored by NMR with 1,3,5-trimethoxybenzene as the internal standard. 3 mL reactor volume. Productivity predicted for a 24-hour reaction period.

With optimized reaction conditions, a small study of substrate scope was carried out by varying the reaction solvent to produce the condensation product of other alkoxy substituents on the furanone, (see Figure 5) where reactions were carried out at 1 M substrate concentration, 200 °C, and 2 mL min^{-1}. As the -R substituent grows in bulk, conversion drops slightly but, overall, the reaction efficiency remains similar. Facile modification of the -R substituent on the alkoxybutenolide is of importance because these substituents influence the properties of coatings produced by the polymerization of the alkoxyfuranones.[20,41]

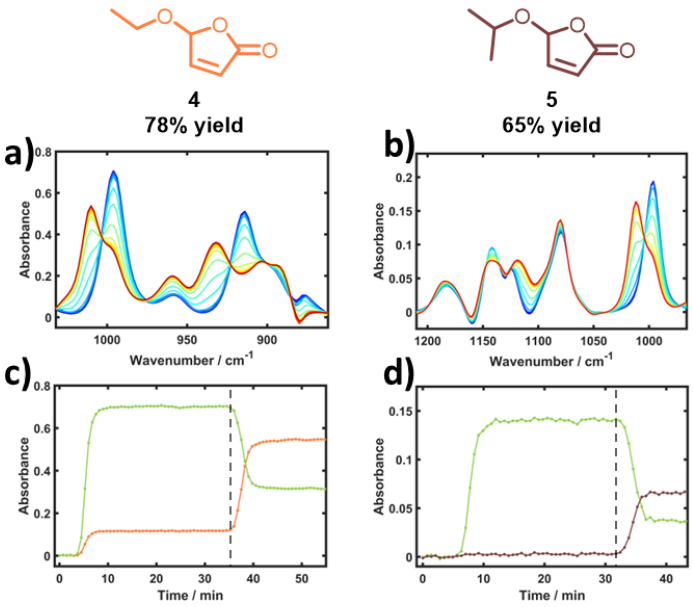

Figure 5. Investigation of additional solvents (EtOH and iPrOH) for the synthesis of alkoxybutenolide monomers 4 & 5. Synthesis was carried out at 200 °C and 2 mL min^{-1} from the optimized conditions from Table 2. a) & b) depict spectral region over time (blue to red). c) & d) are FTIR trends showing the consumption of 5-hydroxyfuranone (green), formation of **4** (orange) and **5** (brown) with the heating turned on indicated by a dotted line.

Telescoped Production of Alkoxybutenolide (3) using Small Scale Taylor Vortex Reactor

To investigate the two reaction steps outlined above in a telescoped flow synthesis, it was necessary to consider the transfer of product from one reactor to another. We used a buffer tank because a peristaltic pump was required at the Vortex outlet due to gas-liquid segmented flow exiting the reactor. This peristaltic pump would be unable to apply suitable head to overcome the high backpressure requirement to superheat methanol to 200 °C. Therefore, a second HPLC pump was used to charge the thermal reactor.

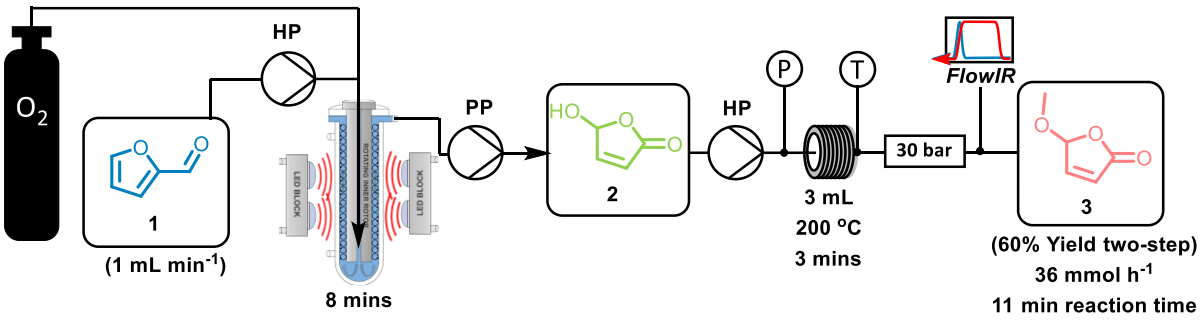

Figure 6. Simplified schematic of the telescoped reaction setup using the small Taylor vortex reactor. HPLC pumps are labelled HP and peristaltic pump is labelled PP. **2** was collected in a buffer tank before being charged into the reactor. Inline FTIR was used at the outlet of the second step to monitor both reactions.

Using the highest yielding conditions from the small-scale vortex reactor, 1 mL min^{-1} and **1** (1 M) were selected for the test of the telescoped reaction (Table 1, entry 2). The photo-oxidation of **1** was carried out in the small-scale vortex reactor for approx. 3 hours to reach steady state and collect material in the buffer tank. The crude product stream was then pumped into the thermal reactor at 1 mL min^{-1}. A 93% yield (NMR) was obtained for the photochemical reaction with an overall two-step yield of 60% for methoxybutenolide, **3**, which corresponds to a slightly reduced second step yield of 65% compared to the pure component reaction (Table 2, entry 7). Even so, this still accounts for a moderate predicted productivity of 36 mmol h^{-1} or 99 g day^{-1} without any intermediate isolation or purification. Both reaction steps were monitored by FTIR at the outlet of the thermal reactor as depicted in Figure 6. Nevertheless, the process was still limited by the photo-oxidation of **1** and the high relative rate of the condensation reaction led us to reinvestigate and scale up the initial photo-oxidation.

Photo-oxidation in the Large Taylor Vortex Reactor

The productivity of the photo-oxidation step in the small vortex reactor was limiting the productivity of the whole telescoped flow synthesis described above. Therefore, our new objective was to further scale up the photo-oxidation of **1** better to match the productivity of the thermal step. Recent advances in scale-up of photochemical reactions both in terms of chemical scope and reactor design have been reviewed.[19,42] We have used our larger-scale PhotoVortex reactor[25] with *ca.* 185 mL irradiated volume and a 2 mm gap width.

Initial reaction conditions were carried out with a jacket temperature of 20 °C, similar to that used above with the small-scale PhotoVortex reactor. Initially, we observed poor reaction efficiencies with low yields at equivalent space times (see Table 3, entries 1 & 2). An interesting observation using

those conditions was that the reactor outlet temperature increased to >40 °C and the methoxylated product **3** was formed thermally in low yields resulting in reduced yields of the desired hydroxybutenolide product, **2**. This could be due to some of the intermediate endoperoxide decomposing thermally back to **1** as suggested by Aubry.[43] We investigated this further using a two-fold strategy: (i) lowering the chiller temperature for the reactor coolant to -5 °C and (ii) precooling the reaction mixture prior to the reactor with a salt-ice bath (ca. -10 °C) and these interventions resulted in the feed solution entering the reactor at between 0 °C and 5 °C. However, the temperatures of the solution at the reactor outlet was still *ca.* 30 °C. With conditions optimized, an 85% yield of **2** (+5% **3**) was achieved with 11.5 mL min^{-1}, providing 570 mmol h^{-1} or 1.3 kg day^{-1}. Higher projected productivities were obtained with 23 mL min^{-1}, 46 mL min^{-1}, and 69 mL min^{-1}, which afforded 1000 mmol h^{-1}(2.4 kg day^{-1}), 1430 mmol h^{-1} (3.4 kg day^{-1}), and 1660 mmol h^{-1} (4.0 kg day^{-1}), respectively (Table 3, entries 4-7).

Table 3. Optimization table for large scale PhotoVortex photo-oxidation of **1** at 1 M.

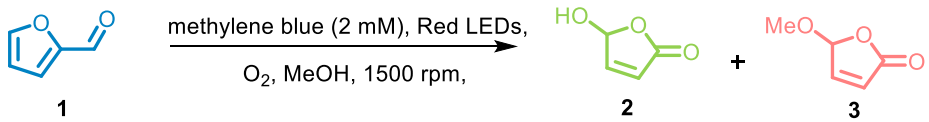

Entry	Chiller Temp (°C)	Spacetime (mins)	Yield of 2 (%)[b]	Yield of 3 (%)[b]	Productivity of 2 (kg day^{-1})[c]	Space time yield (mol h^{-1} mL^{-1})
1	20	8	55	5	1.8	4.1
2	20	4	44	2	2.9	6.6
3	-5	8	61	4	2.0	4.6
4	-5[a]	8	73	2	2.4	5.4
5	-5[a]	16	85	5	1.3	3.2
6	-5[a]	4	52	1	3.4	7.8
7	-5[a]	2.7	40	Trace	4.0	9.0

[a] Feedstock and pre-cooling loop cooled to -10 °C. [b] ^{1}H NMR Yields with 1,3,5-trimethoxybenzene as the internal standard. [c] Predicted productivity over a 24-hour reaction period.

Kilo-Scale Telescoped Flow Synthesis of Methoxybutenolide (3)

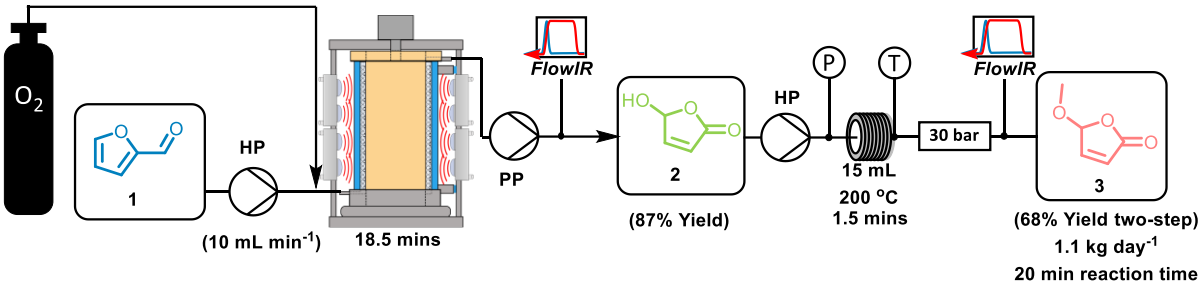

Figure 7. Simplified schematic of the scale up of the telescoped reaction steps towards the synthesis of methoxybutenolide **3**. Pumps are labeled as HP for HPLC pump and PP for peristaltic pump. **2** was collected in a buffer tank before being pumped into the stainless-steel tubing reactor. Pressure and temperature monitors and trips (P and T) were used inline to ensure safe operation. Inline FTIR was also used to ensure that steady state was achieved and showed that the reactions were both stable and robust.

Using the conditions from the telescoped process in the smaller scale Vortex setup, we used the output stream of the large vortex reactor at 10 mL min^{-1} for a proof-of-concept experiment. A 15 mL thermal reactor was used consisting of coiled 1/8" tubing (stainless-steel) to maintain plug flow properties similar to the 3 mL reactor used previously. This resulted in the condensation having a slightly shorter residence time compared to the small-scale telescoped process. Nevertheless, a reaction temperature, 200 °C, was chosen for our investigation. The other conditions were as described in Table 3 with the jacket temperature of the large-scale vortex scale set to -5 °C and feedstock and cooling loop set between -5 to -10 °C. An 87% yield was achieved from the photo-oxidation in the large vortex reactor at 10 mL min^{-1} and with a 400 mL min^{-1} flowrate of O_2. This photo-oxidation product/solution was fed directly into the scaled-up thermal reactor where an overall two-step yield of 68% was achieved with a two-step projected productivity of 1.1 kg day^{-1} being obtained for this telescoped reaction process without any need for intermediate isolation/purification.

CONCLUSION

The reaction steps towards the synthesis of high-performance greener coatings were successfully scaled from 0.03 mol h^{-1} as a thin film batch process to greater than 1.7 mol h^{-1} utilizing a fully continuous PhotoVortex. This equates to a projected productivity of 4 kg day^{-1} in a 24-hour reaction period. This is a thousand-fold increase in productivity compared to 0.0015 mol h^{-1} in the single tubular FEP flow reactor setup which was originally used.[20] We were limited, however, by the distribution of the high flowrates of gas required at increased reaction concentrations which resulted in unstable vortices and reduced reaction yields. We are currently investigating the development of a

high-pressure PhotoVortex which should further enhance the photo-oxidation reactions by increasing the solubility of oxygen but also reducing the flow rate of gas required to satisfy the equivalents of more concentrated reactions. The formation of alkoxybutenolide monomers was accelerated from a 20-hour reflux and scaled to greater than 0.26 mol h^{-1} in a flow-reactor of 3 mL volume, which equates to 732 g day^{-1} for a 24-hour reaction period with residence times of less than 1 minute. This was simply further scaled by increasing the length of tubing which was demonstrated in the scaled telescoped reaction process. Initial tests towards the telescoped reaction scale-up were also investigated which yielded a 0.4 mol h^{-1} or 1.1 kg day^{-1} productivity of the methoxybutenolide without any intermediate purification steps demonstrating viable procedures for ready access to multigram amounts of bio-based monomers for future coating studies.

EXPERIMENTAL SECTION

General Information

All solvents and reagents were used as obtained without any further purification unless stated otherwise. Furfural was distilled under vacuum prior to use. Proton (^{1}H) and Carbon (^{13}C) NMR spectra (Bruker DPX300) (400 MHz and 100 MHz) were recorded at ambient temperatures unless otherwise specified. Chemical shift values are reported in ppm, and solvent resonances were used as internal standards ($CHCl_3$: δ = 7.26 ppm for ^{1}H and 77.16 ppm for ^{13}C). For the yield/conversion, 1,3,5-trimethoxybenzene was used as an internal standard. The spectra were assigned by comparing observed chemical shifts to existing literature values. Column chromatography was carried out using an autocolumn (Teledyne ISCO Next-Gen 300+) with UV (254 nm) or ELS detection. Inline IR analysis was obtained using a Mettler Toledo ReactIR 702L with a 6.3 mm AgX DiComp, all FT-IR spectra were obtained with an air background, spectra were then normalized to the MeOH solvent peak. O_2 was dosed into the reactors using mass flow controllers (MFC) (Bronkhorst) at ambient pressure.

General Reactor Operation – PhotoVortex – Small and Large

The recirculating chiller for cooling the LEDs, was turned on and set to 10 °C whilst the reactor chiller was set to the appropriate temperature for the reaction. The chillers were left to equilibrate for *ca.* 20 min. The reaction mixture was prepared as described below and the inlet tubing for the HPLC pump was fed into the solution and the pump primed. The oxygen cylinder was opened and set to the desired pressure *ca.* 1 bar. The desired flowrate was set on the MFC, and gas dosed into the system at low flowrates (*ca.* 5 mL min^{-1}). The desired liquid flow rate was set on the inlet pump (HPLC or peristaltic) and the solution was pumped into the reactor. The second peristaltic pump for removing

the products from the reactor was set to a flow rate suitably high to pump out the solution from the reactor. The rotation motor of the Vortex reactor was turned on and the speed slowly increased until the desired rotation speed had been achieved. Then the LEDs were turned on at full brightness. The outlet of the peristaltic pump could then be fed into inline FTIR whereby steady state could be monitored and real-time concentrations obtained. If FTIR were not used, two full system volumes were allowed to pass before taking any sample for analysis; this ensured that the reactor had reached a steady state (confirmed by off-line sampling). Once the operation was complete, the LEDs were turned off and the reactor was flushed with pure solvent at increased flowrates to clean the reactor. The inlet pump was turned off, and the rotation speed of the motor was slowly decreased to 0 rpm. The inlet pipe was switched to a container of a compatible solvent (usually the reaction solvent) and the reactor was flushed. The rotation speed was reset during this time to ensure that all material was removed from the reactor. Once the reactor was clean, the motor, pumps, and MFCs were turned off and cylinder isolated. The recirculating chillers were also turned off, provided that the LED blocks were not excessively hot.

General Reaction Conditions – Photo-oxidation of Furfural, 1, in the PhotoVap

Freshly distilled furfural (60 °C, 1 x 10^{-2} bar) was weighed into an appropriately sized volumetric flask for the desired number of experiments. Methylene blue was added to the volumetric flask, and which was topped up with methanol giving the desired catalyst concentration. The solution was homogenized, and the solution was transferred to a vessel, that acted as the feedstock reservoir. If operating semi continuously, the pumps were connected to the Arduino controller and the code for the experiments was generated by modifying serial signal times for the desired application. The MFC was set to bubble O_2 gas into the reactor at 20 mL min^{-1} and the operating Arduino program was initiated. Samples were collected at the outlet pump at the end of each program.

When not operating in a semi-continuous mode, the reactor (1 L round bottom flask) was charged with the desired volume of the reaction mixture (*ca.* 10 mL). The rotation and illumination were manually controlled, and the reaction was carried out for the desired amount of time before replacing the reaction flask manually. The products were analyzed by ^{1}H NMR with 1,3,5-trimethoxybenzene as an internal standard.

General Reaction Conditions – Photo-oxidation of Furfural (1) in the Taylor Vortex Reactor

The furfural and methylene blue solution was prepared as described above for the PhotoVap. Flowrates of O_2 were calculated using the ideal gas law and the MFC was set to the desired setpoints

and the solution of **1** was then pumped into the system for irradiation. After irradiation for the specified amount of time, conditions were either changed or the reactor was flushed with solvent for cleaning. The products were analyzed by ^{1}H NMR with trimethoxybenzene as an internal standard. Methylene blue was removed by trapping with activated charcoal and filtration through Celite. For lower yielding experiments, <75%, unreacted furfural was removed *via* column chromatography (silica gel *n*-pentane:ethyl acetate (90:10) before the product was recrystallized from $CHCl_3$ by seeding. For higher-yielding experiments, the product could be directly recrystallized by seeding a supersaturated solution and cooling it in the freezer (-20°) before filtering to collect product **2** as a white solid.

General Reaction Conditions – Thermal Condensation of (2) with R-OH to the Corresponding Alkoxybutenolide

A solution of 5-hydroxyfuranone, **2**, (0.1 - 1 M) was prepared in an appropriately sized volumetric flask with the desired alcohol solvent. The solution was homogenized and transferred to the HPLC pump for priming. Initially pure solvent was pumped through the reactor and the backpressure regulator was set to the required pressure setpoint. The reactor was heated to the desired temperature and a valve was opened to allow the reaction solution to be pumped into the reactor. Samples were taken once steady state was achieved and reaction conditions (temperature or flowrate) were changed when screening was the objective. When the experiment was completed, the reactor was flushed with pure solvent to clean the system after which the temperature was reduced to ambient and backpressure released. The product yields were analyzed by ^{1}H NMR with trimethoxybenzene as an internal standard. Alkoxybutenolide isolation was carried out *via* column chromatography (silica gel *n*-pentane:ethyl acetate (90:10)) to purify the products **3-5** as colorless oils.

General Reaction Conditions – Telescoped flow synthesis

The reaction mixture of **1** and methylene bule was prepared as before and the O_2 gas flow rate was set as above. The solution of **1,** was then pumped into the system for irradiation. Once steady-state was reached, the output of the photo-reactor was pumped into a buffer tank where it was collected before being pumped into the pressurized thermal reactor. The yield of **2,** was calculated by analyzing the contents of the buffer tank using 1,3,5-trimethoxybenzene as an internal standard. The inlet pump (HPLC) for the thermal reaction was primed and the solution of **2** was pumped from the buffer tank into the thermal reactor. The back pressure regulator and then heating block were set to their desired setpoints. The products were collected in an appropriately sized waste container where the final product **3**, was collected. The overall yield of the two-step process was calculated using ^{1}H

NMR with 1,3,5-trimethoxybenzene as the internal standard. The PhotoVortex and thermal reactors were cleaned separately following the general procedures outlined above.

Acknowledgments: We are grateful for funding by UKRI Programme Grant [EP/P013341/1], the University of Nottingham EPSRC Impact Acceleration Account and the EPSRC and SFI Centre for Doctoral Training in Sustainable Chemistry: Atoms-2-Products an Integrated Approach to Sustainable Chemistry [EP/S022236/1] (for HA, RL, IM and MTP) and AstraZeneca for support to MTP. BLF acknowledges the Advanced Research Center for Chemical Building Blocks, ARC CBBC, which is cofounded and co-financed by the Netherlands Organization for Scientific Research (NWO, contract 736.000.000) and the Netherlands Ministry of Economic Affairs and Climate We thank Ben Clarke, Richard Wilson, Richard Meehan, Matthew McAdam, David Lichfield, Martin Dellar, and Mark Guyler for their outstanding technical support at the School of Chemistry, UoN. The data created by this research are available in the ESI.

Conflicts of Interest

The authors declare no conflicts of interest.

References

(1) Cabernard, L.; Pfister, S.; Oberschelp, C.; Hellweg, S. Growing Environmental Footprint of Plastics Driven by Coal Combustion. *Nat Sustain* **2021**, *5*, 139–148. DOI:10.1038/s41893-021-00807-2.

(2) Rosenboom, J.-G.; Langer, R.; Traverso, G. Bioplastics for a Circular Economy. *Nat Rev Mater* **2022**, *7*, 117–137. DOI:10.1038/s41578-021-00407-8.

(3) Goyal, S.; Hernández, N. B.; Cochran, E. W. An Update on the Future Prospects of Glycerol Polymers. *Polymer International* **2021**, *70*, 911–917. DOI:10.1002/pi.6209.

(4) Della Monica, F.; Kleij, A. W. From Terpenes to Sustainable and Functional Polymers. *Polym. Chem.* **2020**, *11*, 5109–5127. DOI:10.1039/D0PY00817F.

(5) Sainz, M. F.; Souto, J. A.; Regentova, D.; Johansson, M. K. G.; Timhagen, S. T.; Irvine, D. J.; Buijsen, P.; Koning, C. E.; Stockman, R. A.; Howdle, S. M. A Facile and Green Route to Terpene Derived Acrylate and Methacrylate Monomers and Simple Free Radical Polymerisation to Yield New Renewable Polymers and Coatings. *Polym. Chem.* **2016**, *7*, 2882–2887. DOI:10.1039/C6PY00357E.

(6) Cuzzucoli Crucitti, V.; Ilchev, A.; Moore, J. C.; Fowler, H. R.; Dubern, J.-F.; Sanni, O.; Xue, X.; Husband, B. K.; Dundas, A. A.; Smith, S.; Wildman, J. L.; Taresco, V.; Williams, P.; Alexander, M. R.; Howdle, S. M.; Wildman, R. D.; Stockman, R. A.; Irvine, D. J. Predictive Molecular Design and Structure–Property Validation of Novel Terpene-Based, Sustainably Sourced Bacterial Biofilm-Resistant Materials. *Biomacromolecules* **2023**, *24*, 576–591. DOI:10.1021/acs.biomac.2c00721.

(7) Birajdar, M. S.; Joo, H.; Koh, W.-G.; Park, H. Natural Bio-Based Monomers for Biomedical Applications: A Review. *Biomater Res* **2021**, *25*, 8. DOI:10.1186/s40824-021-00208-8.

(8) Lligadas, G.; Ronda, J. C.; Galià, M.; Cádiz, V. Renewable Polymeric Materials from Vegetable Oils: A Perspective. *Materials Today* **2013**, *16*, 337–343. DOI:10.1016/j.mattod.2013.08.016.

(9) Anwar, Z.; Gulfraz, M.; Irshad, M. Agro-Industrial Lignocellulosic Biomass a Key to Unlock the Future Bio-Energy: A Brief Review. *Journal of Radiation Research and Applied Sciences* **2014**, *7*, 163–173. DOI:10.1016/j.jrras.2014.02.003.

(10) Preethi; M., G.; Kumar, G.; Karthikeyan, O. P.; Varjani, S.; J., R. B. Lignocellulosic Biomass as an Optimistic Feedstock for the Production of Biofuels as Valuable Energy Source: Techno-Economic Analysis, Environmental Impact Analysis, Breakthrough and Perspectives. *Environmental Technology & Innovation* **2021**, *24*, 102080. DOI:10.1016/j.eti.2021.102080.

(11) Veith, C.; Diot-Néant, F.; Miller, S. A.; Allais, F. Synthesis and Polymerization of Bio-Based Acrylates: A Review. *Polym. Chem.* **2020**, *11*, 7452–7470. DOI:10.1039/D0PY01222J.

(12) Samyn, P.; Bosmans, J.; Cosemans, P. Comparative Study on Mechanical Performance of Photocurable Acrylate Coatings with Bio-Based versus Fossil-Based Components. *Materials Today Communications* **2022**, *32*, 104002. DOI:10.1016/j.mtcomm.2022.104002.

(13) Jaswal, A.; Singh, P. P.; Mondal, T. Furfural – a Versatile, Biomass-Derived Platform Chemical for the Production of Renewable Chemicals. *Green Chem.* **2022**, *24*, 510–551. DOI:10.1039/D1GC03278J.

(14) Bozell, J. J.; Petersen, G. R. Technology Development for the Production of Biobased Products from Biorefinery Carbohydrates—the US Department of Energy's "Top 10" Revisited. *Green Chem.* **2010**, *12*, 539. DOI:10.1039/b922014c.

(15) Hermens, J. G. H.; Freese, T.; Alachouzos, G.; Lepage, M. L.; Van Den Berg, K. J.; Elders, N.; Feringa, B. L. A Sustainable Polymer and Coating System Based on Renewable Raw Materials. *Green Chem.* **2022**, *24*, 9772–9780. DOI:10.1039/D2GC03657F.

(16) Hermens, J. G. H.; Jensma, A.; Feringa, B. L. Highly Efficient Biobased Synthesis of Acrylic Acid. *Angew Chem Int Ed* **2022**, *61*, e202112618. DOI:10.1002/anie.202112618.

(17) Feringa, B. L. Photo-Oxidation of Furans. *Recl. Trav. Chim. Pays-Bas* **1987**, *106*, 469–488. DOI:10.1002/recl.19871060902.

(18) ECHEMI. *The Global Acrylic Market Is Accelerating Its Transfer to China*. https://www.echemi.com/cms/603798.html.

(19) Donnelly, K.; Baumann, M. Scalability of Photochemical Reactions in Continuous Flow Mode. *J Flow Chem* **2021**, *11*, 223–241. DOI:10.1007/s41981-021-00168-z.

(20) Hermens, J. G. H.; Freese, T.; van den Berg, K. J.; van Gemert, R.; Feringa, B. L. A Coating from Nature. *Sci. Adv.* **2020**, *6*, eabe0026. DOI:10.1126/sciadv.abe0026.

(21) Brzozowski, M.; O'Brien, M.; Ley, S. V.; Polyzos, A. Flow Chemistry: Intelligent Processing of Gas–Liquid Transformations Using a Tube-in-Tube Reactor. *Acc. Chem. Res.* **2015**, *48*, 349–362. DOI:10.1021/ar500359m.

(22) Hermens, J. G. H.; Lepage, M. L.; Kloekhorst, A.; Keller, E.; Bloem, R.; Meijer, M.; Feringa, B. L. Development of a Modular Photoreactor for the Upscaling of Continuous Flow Photochemistry. *React. Chem. Eng.* **2022**, *7*, 2280–2284. DOI:10.1039/D2RE00310D.

(23) Chaudhuri, A.; Zondag, S. D. A.; Schuurmans, J. H. A.; Van Der Schaaf, J.; Noël, T. Scale-Up of a Heterogeneous Photocatalytic Degradation Using a Photochemical Rotor–Stator Spinning Disk Reactor. *Org. Process Res. Dev.* **2022**, *26*, 1279–1288. DOI:10.1021/acs.oprd.2c00012.

(24) Lee, D. S.; Amara, Z.; Clark, C. A.; Xu, Z.; Kakimpa, B.; Morvan, H. P.; Pickering, S. J.; Poliakoff, M.; George, M. W. Continuous Photo-Oxidation in a Vortex Reactor: Efficient Operations Using Air Drawn from the Laboratory. *Org. Process Res. Dev.* **2017**, *21*, 1042–1050. DOI:10.1021/acs.oprd.7b00153.

(25) Lee, D. S.; Sharabi, M.; Jefferson-Loveday, R.; Pickering, S. J.; Poliakoff, M.; George, M. W. Scalable Continuous Vortex Reactor for Gram to Kilo Scale for UV and Visible Photochemistry. *Org. Process Res. Dev.* **2020**, *24*, 201–206. DOI:10.1021/acs.oprd.9b00475.

(26) Luyben, W. L. Temperature Setpoint-Ramp Control Structure for Batch Reactors. *Chemical Engineering Science* **2019**, *208*, 115124. DOI:10.1016/j.ces.2019.07.042.

(27) Adeyemi, A.; Bergman, J.; Brånalt, J.; Sävmarker, J.; Larhed, M. Continuous Flow Synthesis under High-Temperature/High-Pressure Conditions Using a Resistively Heated Flow Reactor. *Org. Process Res. Dev.* **2017**, *21*, 947–955. DOI:10.1021/acs.oprd.7b00063.

(28) Donnelly, K.; Baumann, M. Continuous Flow Technology as an Enabler for Innovative Transformations Exploiting Carbenes, Nitrenes, and Benzynes. *J. Org. Chem.* **2022**, *87*, 8279–8288. DOI:10.1021/acs.joc.2c00963.

(29) Razzaq, T.; Glasnov, T. N.; Kappe, C. O. Continuous-Flow Microreactor Chemistry under High-Temperature/Pressure Conditions. *Eur. J. Org. Chem.* **2009**, 1321–1325. DOI:10.1002/ejoc.200900077.

(30) Mallia, C. J.; McCreanor, N. G.; Legg, D. H.; Stewart, C. R.; Coppock, S.; Ashworth, I. W.; Le Bars, J.; Clarke, A.; Clemens, G.; Fisk, H.; Benson, H.; Oke, S.; Churchill, T.; Hoyle, M.; Timms, L.; Vare, K.; Sims, M.; Knight, S. Development and Manufacture of a Curtius Rearrangement Using Continuous Flow towards the Large-Scale Manufacture of AZD7648. *Org. Process Res. Dev.* **2022**, *26*, 3312–3322. DOI:10.1021/acs.oprd.2c00316.

(31) Hessel, V.; Kralisch, D.; Kockmann, N.; Noël, T.; Wang, Q. Novel Process Windows for Enabling, Accelerating, and Uplifting Flow Chemistry. *ChemSusChem* **2013**, *6*, 746–789. DOI:10.1002/cssc.201200766.

(32) Znidar, D.; O'Kearney-McMullan, A.; Munday, R.; Wiles, C.; Poechlauer, P.; Schmoelzer, C.; Dallinger, D.; Kappe, C. O. Scalable Wolff–Kishner Reductions in Extreme Process Windows Using a Silicon Carbide Flow Reactor. *Org. Process Res. Dev.* **2019**, *23*, 2445–2455. DOI:10.1021/acs.oprd.9b00336.

(33) Howie, R. A.; Elliott, L. D.; Kayal, S.; Sun, X.-Z.; Hanson-Heine, M. W. D.; Hunter, J.; Clark, C. A.; Love, A.; Wiseall, C.; Lee, D. S.; Poliakoff, M.; Booker Milburn, K. I.; George, M. W. Integrated Multistep Photochemical and Thermal Continuous Flow Reactions: Production of Bicyclic Lactones with Kilogram Productivity. *Org. Process Res. Dev.* **2021**, *25*, 2052–2059. DOI:10.1021/acs.oprd.1c00089.

(34) Baumann, M.; Moody, T. S.; Smyth, M.; Wharry, S. Evaluating the Green Credentials of Flow Chemistry towards Industrial Applications. *Synthesis* **2021**, *53*, 3963–3976. DOI:10.1055/a-1541-1761.

(35) Clark, C. A.; Lee, D. S.; Pickering, S. J.; Poliakoff, M.; George, M. W. A Simple and Versatile Reactor for Photochemistry. *Org. Process Res. Dev.* **2016**, *20*, 1792–1798. DOI:10.1021/acs.oprd.6b00257.

(36) Noda, I.; Ozaki, Y. *Two-Dimensional Correlation Spectroscopy Applications in Vibrational and Optical Spectroscopy*; Wiley, 2004.

(37) Love, A.; Lee, D. S.; Gennari, G.; Jefferson-Loveday, R.; Pickering, S. J.; Poliakoff, M.; George, M. A Continuous-Flow Electrochemical Taylor Vortex Reactor: A Laboratory-Scale High-Throughput Flow Reactor with Enhanced Mixing for Scalable Electrosynthesis. *Org. Process Res. Dev.* **2021**, *25*, 1619–1627. DOI:10.1021/acs.oprd.1c00102.

(38) Lee, D. S.; Love, A.; Mansouri, Z.; Waldron Clarke, T. H.; Harrowven, D. C.; Jefferson-Loveday, R.; Pickering, S. J.; Poliakoff, M.; George, M. W. High-Productivity Single-Pass Electrochemical Birch Reduction of Naphthalenes in a Continuous Flow Electrochemical Taylor Vortex Reactor. *Org. Process Res. Dev.* **2022**, *26*, 2674–2684. DOI:10.1021/acs.oprd.2c00108.

(39) *Reaction Lab Software Information - Scale-up Systems*. https://www.scale-up.com/ReactionLab.

(40) Hone, C. A.; Holmes, N.; Akien, G. R.; Bourne, R. A.; Muller, F. L. Rapid Multistep Kinetic Model Generation from Transient Flow Data. *React. Chem. Eng.* **2017**, *2*, 103–108. DOI:10.1039/C6RE00109B.

(41) Lepage, M. L.; Alachouzos, G.; Hermens, J. G. H.; Elders, N.; Van Den Berg, K. J.; Feringa, B. L. Electron-Poor Butenolides: The Missing Link between Acrylates and Maleic Anhydride in Radical Polymerization. *J. Am. Chem. Soc.* **2023**, *145*, 17211–17219. DOI:10.1021/jacs.3c04314.

(42) Zondag, S. D. A.; Mazzarella, D.; Noël, T. Scale-Up of Photochemical Reactions: Transitioning from Lab Scale to Industrial Production. *Annu. Rev. Chem. Biomol. Eng.* **2023**, *14*, 283–300. DOI:10.1146/annurev-chembioeng-101121-074313.

(43) Aubry, J.-M.; Pierlot, C.; Rigaudy, J.; Schmidt, R. Reversible Binding of Oxygen to Aromatic Compounds. *Acc. Chem. Res.* **2003**, *36*, 668–675. DOI:10.1021/ar010086g.